two of the short ring 1 distances (N_5–O_{11}' = 2.895 Å and N_5–O_7 = 2.862 Å) are between the same exocyclic nitrogen atom and two nonbridging oxygen atoms. The corresponding distances of ring 2 (N_9–O_8' = 3.121 Å and N_9–O_{12} = 2.852 Å) involve one double bridging oxygen (O_8') atom and one single bridging oxygen (O_{12}) atom. In general, the corresponding closest approach distances for hydrogen bonding from the two melaminium cations are significantly different.

The melaminium cations are extensively hydrogen bonded to the molybdate anions and to adjacent cations. This extensive hydrogen bonding acts in concert with the crystalline lattice forces to account for both the unique configuration of β-$Mo_8O_{26}^{4-}$ and the nonequivalency of the crystallographically independent melaminium cations as found in $(Hmel)_4Mo_8O_{26}$. It also provides an explanation for the high thermal stability (260 °C) of this species.

Hydrogen bonding also plays a role in determining the structure of β-$Mo_8O_{26}^{4-}$ in $(NH_4)_4Mo_8O_{26}\cdot 4H_2O$[4] and (3-Etpy)$_4Mo_8O_{26}$.[1] In the case of the nonhydrated (3-Etpy)$_4Mo_8O_{26}$, the structure is characterized by infinite chains of polyanions bridged by one of the two crystallographically independent 3-ethylpyridinium cations through hydrogen bonds with the molybdate anions.[1] While the other cation does not contribute directly to the chain formation, it apparently does hydrogen bond to a molybdate oxygen atom.[1]

The ammonium ions and the water of crystallization in $(NH_4)_4Mo_8O_{26}\cdot 4H_2O$ are positioned to extensively hydrogen bond with each other as well as with molybdate oxygen atoms.[4] In light of this extensive hydrogen bonding in all three of the β-$Mo_8O_{26}^{4-}$ structures discussed, we believe it likely that hydrogen bonding plays an important role in determining the solid-state structures of most amine molybdates and organoammonium molybdates and influences their chemical and physical properties.

Acknowledgment. The National Science Foundation is acknowledged for purchase of the Syntex diffractometer at Case Western Reserve University.

Registry No. $(HMel)_4Mo_8O_{26}$, 65036-95-5.

Supplementary Material Available: Tables of anisotropic parameters and observed and calculated structure factor amplitudes and figures of the melaminium cation, the β-octamolybdate anion, and the cluster melaminium cations (13 pages). Ordering information is given on any current masthead page.

Contribution from the Department of Chemistry, Faculty of Engineering Science, and Department of Macromolecular Science, Faculty of Science, Osaka University, Toyonaka, Osaka 560, Japan, Department of Chemistry, Faculty of Science, Osaka City University, Sumiyoshi-ku, Osaka 558, Japan, and Laboratory of Natural Products Chemistry, Tokushima Research Institute, Otsuka Pharmaceutical Company Ltd., Kawauchi-cho, Tokushima 771-01, Japan

X-ray Crystallographic, Spectral, and Molecular Orbital Studies on Molybdenum(II) Acetylene Complexes, Mo(*t*-BuS)$_2$(*t*-BuNC)$_2$(RC≡CR') (R, R' = H or Ph)

M. KAMATA,[1a] K. HIROTSU,[1b] T. HIGUCHI,*[1b] M. KIDO,[1c] K. TATSUMI,*[1d] T. YOSHIDA,[1a] and SEI OTSUKA*[1a]

Received September 8, 1982

Facile substitution reactions of a bis(thiolato) Mo(II) complex, *cis*-Mo(*t*-BuS)$_2$(*t*-BuNC)$_4$, with acetylenes (HC≡CH, PhC≡CH, and PhC≡CPh) occur to give acetylene compounds of general formula Mo(*t*-BuS)$_2$(*t*-BuNC)$_2$(RC≡CR') (**1**, R = R' = H; **2**, R = H, R' = Ph; **3**, R = R' = Ph) in substantial yields (>60%). Compound **1** crystallizes in a monoclinic cell of dimensions a = 18.672 (9) Å, b = 10.105 (3) Å, c = 17.322 (8) Å, and β = 112.58 (7)° with Z = 4 in space group $P2_1/a$. Refinement by block-diagonal least-squares methods on F, employing 1685 diffractometer data, converged at R = 0.059. Compound **3** also crystallizes in a monoclinic space group, $P2_1/c$, with Z = 4 in a unit cell of dimensions a = 16.982 (9) Å, b = 17.378 (8) Å, c = 12.013 (6) Å, and β = 96.59 (4)°. A total of 2694 unique intensity data were used for block-diagonal least-squares refinement on F, which converged at R = 0.062. The molecules **1** and **3** assume approximately trigonal-bipyramidal geometry with acetylene considered as a unidentate ligand. The triple bond lies almost parallel to the main molecular axis. The C≡C, mean Mo—C≡, and mean Mo–S bond distances are respectively 1.28 (2), 2.05 (2), and 2.325 (3) Å for **1** and 1.28 (2), 2.054 (7), and 2.338 (2) Å for **3**. The same molecular geometry can be inferred for **2** on the basis of the spectroscopic data, inter alia the ^{1}H NMR spectrum. The ^{1}H NMR spectra of **1**–**3** also indicated their stereochemical rigidity in solution up to about 100 °C. Extended Hückel molecular orbital calculations were performed on the simplified molecule Mo(HS)$_2$(HNC)$_2$(HC≡CH) in nine possible geometrical variations to find (1) the preferred orientation of the acetylene, (2) the preferred orientation of the thiolates, and (3) the site preference of the ligands, i.e. axial vs. equatorial. The most theoretically stable molecular configuration coincides with what was established by the present X-ray analysis. The nature of the metal–acetylene bonds was elucidated from the molecular geometries, and from IR and ^{1}H NMR spectra, and these findings were rationalized by an EHMO analysis.

Molybdenum compounds of sulfur ligands have attacted considerable interest in recent years because of their possible implications for redox enzyme chemistry.[2,3] In particular, the coordination of alkynes, an enzymic substrate, is the subject of a number of recent papers. As a Mo(IV) acetylene complex, only MoO(dtc)$_2$(RC≡CR') (dtc = dialkyldithiocarbamato) is known.[4] While several types of Mo(II) alkyne complexes have been reported, they are confined essentially to those carrying an η-C_5H_5 (Cp) group(s), MoX(Cp)(RC≡CR)$_2$,[5] MoX(Cp)(CO)(RC≡CR),[5,6] Mo(Cp)(dpe)(RC≡CR)[7] (dpe = (diphenylphosphino)ethane), Mo(Cp)(CO)(RC≡CR)$_2^+$,[8]

(1) (a) Department of Chemistry, Osaka University. (b) Osaka City University. (c) Otsuka Pharmaceutical Co. Ltd. (d) Department of Macromolecular Science, Osaka University.
(2) (a) Newton, W. E., Otsuka, S., Eds., "Molybdenum Chemistry of Biological Significance"; Plenum Press: New York, 1980. (b) Kuehn, C. G.; Isied, S. S. *Prog. Inorg. Chem.* **1980**, *27*, 153–221.
(3) Cramer, S. P.; Wahl, R.; Rajagopalan, K. V. *J. Am. Chem. Soc.* **1981**, *103*, 7721–7727 and references therein.
(4) (a) Maatta, E. A.; Wentworth, R. A. D.; Newton, W. E.; McDonald, J. W.; Watt, G. D. *J. Am. Chem. Soc.* **1978**, *100*, 1320–1321. (b) Newton, W. E.; McDonald, J. W.; Corbin, J. S.; Ricard, L.; Weiss, R. *Inorg. Chem.* **1980**, *19*, 1997–2006.
(5) (a) Davidson, J. L.; Sharp, D. W. A. *J. Chem. Soc., Dalton Trans.* **1975**, 2531–2534. (b) Faller, J. W.; Murray, H. H. *J. Organomet. Chem.* **1979**, *172*, 171–176.
(6) Davidson, J. L.; Green, M.; Stone, F. G. A.; Welch, A. J. *J. Chem. Soc., Dalton Trans.* **1976**, *738*–745.
(7) Green, M. L. H.; Knight, J.; Segal, J. A. *J. Chem. Soc., Dalton Trans.* **1977**, 2189–2195.
(8) Watson, P. L.; Bergman, R. G. *J. Am. Chem. Soc.* **1980**, *102*, 2698–2703.

0020-1669/83/1322-2416$01.50/0

$Mo(Cp)_2(RC{\equiv}CR')$,[9a] and $Mo(SC_6F_5)(Cp)(CO)(RC{\equiv}CR)$,[10a] or carrying a chelating disulfur ligand(s), $M(dtc)_2(CO)(RC{\equiv}CR')$ (M = Mo, W)[11] and $Mo[S_2P(i\text{-}Pr)_2]_2(CO)(RC{\equiv}CR')$.[12] Also Mo(TPP)(RC≡CR) (TPP = tetraphenylporphyrin) is known.[9b] A couple of Mo(I) dimeric compounds, $Mo_2(Cp)_2(\mu\text{-}RC{\equiv}CR')$[13] and $Mo_2(Cp)_2(CO)_4(\mu\text{-}C_2H_2)$,[14] have been reported, and M(0) compounds, $M(CO)(PhC{\equiv}CPh)_3$ (M = Mo, W), have also been prepared.[15]

Recently we have prepared a mononuclear Mo(II) thiolate compound, $Mo(t\text{-}BuS)_2(t\text{-}BuNC)_4$, from $Mo(t\text{-}BuS)_4$[16] and established the molecular structure by X-ray crystallography.[17] This compound is chemically significant in several respects: (1) it is a unique example of a Mo(II) ion containing biologically important, simple thiolate ligands, (2) it can be regarded as a coordinatively unsaturated, 16-electron system, and related to this, (3) in solution it exhibits high reactivity toward π-acids and oxidizing agents, yet in the solid state it is fairly air insensitive, permitting aerobic handling for a short while. Two reaction schemes were anticipated for the reaction of $Mo(t\text{-}BuS)_2(t\text{-}BuNC)_4$ with a π-acid such as acetylene: reduction elimination of *t*-BuS ligands leading to lower valent complexes or substitution of *t*-BuNC ligands with the π-acid. We found that, with the representative acetylenes HC≡CH, PhC≡CH, and PhC≡CPh, the latter reaction occurs selectively, producing Mo(II) acetylene complexes of formula $Mo(t\text{-}BuS)_2(t\text{-}BuNC)_2(RC{\equiv}CR')$ (R = R′ = H, **1**; R = H, R′ = Ph, **2**; R = R′ = Ph, **3**).[18]

It is rather surprising to find that so far only a few mononuclear Mo alkyne complexes, $MoO(dtc)_2(ArC{\equiv}CAr)$,[4c] $MoO(Cp)(SC_6F_5)(CF_3C{\equiv}CCF_3)$,[10b] $Mo(dtc)_2(CO)(RC{\equiv}CR')$ (R = H, Ph),[11] $Mo(SC_6F_5)(Cp)(CO)(CF_3{\equiv}CCF_3)$,[10b] and Mo(TPP)(PhC≡CPh),[9b] have undergone X-ray structural analysis. Thus, compounds **1–3** deserve structural studies. Also their rather simple molecular structure presents an object amenable to theoretical studies of the molecular geometry and the nature of alkyne coordination bonding. The alkyne–metal bonding in early transition metal compounds may involve electron donation from the alkyne π-bond to the metal,[19] in addition to the familiar dπ–pπ back-bonding. The pπ donation was considered to be of primary importance in the alkyne–metal interactions and a formalism of numbers (2–4) of electrons donated per alkyne ligands was invoked in order to account for the alkyne ^{13}C NMR shift data observed for a series of the Mo(II) and W(II) complexes.[11c] This view is based on the inert-gas rule and also on theoretical calculations with the extended Hückel approximation. Since the empirical rule has been a subject of criticism[20,21] and, furthermore, because sulfur is involved in redox-active molybdoenzymes,[3,22,23] we were particularly interested in obtaining chemical information on the role of simple thiolate ligands in the alkyne coordination to a Mo center.

Table I. Summary of Crystal Data and Intensity Collection for $Mo(t\text{-}BuS)_2(t\text{-}BuNC)_2(HC{\equiv}CH)\cdot{}^1/_2C_6H_{14}$ (1) and $Mo(t\text{-}BuS)_2(t\text{-}BuNC)_2(PhC{\equiv}CPh)$ (3)

	1	3
A. Crystal Parameters		
cryst size, mm	0.30 × 0.21 × 0.35	0.41 × 0.22 × 0.20
cryst habit	prism	prism
a, Å	18.672 (9)	16.982 (9)
b, Å	10.105 (3)	17.378 (8)
c, Å	17.322 (8)	12.013 (6)
β, deg	112.58 (7)	96.59 (4)
V, Å^3	3018 (3)	3522
Z	4	4
cryst syst	monoclinic	monoclinic
space group	$P2_1/a$	$P2_1/c$
ρ(calcd), g cm^{-3}	1.12	1.17
fw	509.68	618.79
μ, cm^{-1}	5.57	4.88
B. Measurements of Intensity Data		
diffractometer	PW1100 (Philips)	Syntex R_3
radiation (graphite monochromated)	Mo Kα	Mo Kα
temp, °C	18	20
scan mode	$\theta{:}2\theta$	ω
scan range, deg	4–44	3–40
data collection range	±*h*,*k*,*l*	±*h*,*k*,*l*
scan rate, deg min^{-1}	2.0	3–30 (limits)
scan width, deg	1.5 + 0.3 tan θ	1
bkgd time/scan time	1.0	1.0
std reflctns	3 every 3 h, no decay obsd	3 every 97 refs, no decay obsd
no. of unique data collected	2780	3196
no. of unique data used	1685 ($I > 3\sigma(I)$)	2694 ($I > 2\sigma(I)$)

Experimental Section

^1H and ^{13}C NMR spectra were recorded with JEOL JNM-PMX-60 and JNM-FX-100 instruments. IR and electronic spectra were measured with Hitachi Model 295 and Hitachi Model EPS-3T spectrometers, respectively. All reactions and manipulations were carried out under a nitrogen atmosphere. $Mo(t\text{-}BuS)_2(t\text{-}BuNC)_4$ was prepared from $Mo(t\text{-}BuS)_4$[16] by the method reported previously.[17] Commerical acetylene (Fuji Gas Kogyo Co. Ltd.) was employed after standard purification. PhC≡CPh and PhC≡CH were prepared by literature methods.

Preparation of $Mo(t\text{-}BuS)_2(t\text{-}BuNC)_2(HC{\equiv}CH)$ (1). Into a flask containing a solution of $Mo(t\text{-}BuS)_2(t\text{-}BuNC)_4$ (0.5 mmol) dissolved in toluene (20 mL) a gentle stream of acetylene was introduced with stirring for 80 min at 30 °C. During this time the initial deep yellow-green solution slowly turned to red. Solvent removal under vacuum left a red oil. The red oil was then chromatographed on a short alumina column with *n*-hexane as the eluent to yield a red solution. The volume was reduced to 3 mL and cooled at −30 °C overnight to give orange-vermilion crystals of **1**: yield 0.32 mmol, 63%; mp 120 °C. Anal. ($C_{20}H_{38}N_2S_2Mo$) C, H, N.

Preparation of $Mo(t\text{-}BuS)_2(t\text{-}BuNC)_2(PhC{\equiv}CH)$ (2). To a solution of $Mo(t\text{-}BuS)_2(t\text{-}BuNC)_4$ (0.5 mmol) dissolved in toluene (20 mL) was added with stirring PhC≡CH (excess), and stirring was continued at 50 °C for 1 h. The resulting red solution was evaporated

(9) (a) Thomas, J. L. *Inorg. Chem.* **1978**, *17*, 1507–1511. (b) De Ciau, A.; Colin, J.; Schappacher, M.; Ricard, L.; Weiss, R. *J. Am. Chem. Soc.* **1981**, *103*, 1850–1851.
(10) (a) Braterman, P. S.; Davidson, J. L.; Sharp, D. W. A. *J. Chem. Soc., Dalton Trans.* **1976**, 241–245. (b) Howard, J. A. K.; Stansfield, R. F. D.; Woodward, P. *Ibid.* **1976**, 246–250.
(11) (a) McDonald, J. W.; Newton, W. E.; Grredy, C. T.; Corbin, J. L. *J. Organomet. Chem.* **1975**, *92*, C25–27. (b) Ricard, L.; Weiss, R.; Newton, W. E. Chew, G. J.-J.; McDonald, J. W. *J. Am. Chem. Soc.* **1978**, *100*, 1318–1320. (c) Templeton, J. L.; Ward, B. C. *Ibid.* **1980**, *102*, 1532–1538, 3288–3290. (d) Templeton, J. L.; Winston, P. B.; Ward, B. C. *Ibid.* **1981**, *103*, 7713–7721.
(12) McDonald, J. W.; Corbin, J. L.; Newton, W. E. *J. Am. Chem. Soc.* **1975**, *97*, 1970–1971.
(13) (a) Nakamura, A.; Hagihara, N. *Nippon Kagaku Zasshi* **1963**, *84*, 344–348. (b) Nakamura, A. *Mem. Inst. Sci. Ind. Res., Osaka Univ.* **1962**, *19*, 81–95.
(14) Baily, W. I., Jr.; Chisholm, M. H.; Cotton, F. A.; Rankel, L. A. *J. Am. Chem. Soc.* **1978**, *100*, 5764–5773.
(15) (a) Strohmeier, W.; von Hobe, D. *Z. Naturforsch., B: Anorg. Chem., Org. Chem., Biochem., Biophys., Biol.* **1964**, *19B*, 959–960. (b) King, R. B. *Inorg. Chem.* **1968**, *7*, 1044–1046.
(16) Otsuka, S.; Kamata, M.; Hirotsu, K.; Higuchi, T. *J. Am. Chem. Soc.* **1981**, *103*, 3011–3014.
(17) (a) Kamata, M.; Yoshida, T.; Otsuka, S.; Hirotsu, K.; Higuchi, T. *J. Am. Chem. Soc.* **1981**, *103*, 3572–3574. (b) Kamata, M.; Hirotsu, K.; Higuchi, T.; Tatsumi, K.; Yoshida, T.; Hoffmann, R.; Otsuka, S. *Ibid.* **1981**, *103*, 5722–5778.
(18) Kamata, M.; Yoshida, T.; Otsuka, S.; Hirotsu, K.; Higuchi, T.; Kido, M.; Tatsumi, K.; Hoffmann, R. *Organometallics* **1982**, *1*, 227–230.
(19) Otsuka, S.; Nakamura, A. *Adv. Organomet. Chem.* **1976**, *14*, 245–279.
(20) Mingos, D. M. P. *Adv. Organomet. Chem.* **1977**, *15*, 1–51.
(21) Craig, D. P.; Doggett, G. *J. Chem. Soc.* **1963**, *4189*–4198.
(22) Stiefel, E. I. *Prog. Inorg. Chem.* **1977**, *22*, 1–223.
(23) Spence, J. T. *Met. Ions Biol. Syst.* **1976**, *5*, 280–321.

Table II. Fractional Coordinates for $Mo(t\text{-BuS})_2(t\text{-BuNC})_2(HC{\equiv}CH)\cdot{}^1/_2C_6H_{14}$[a]

atom	x	y	z
Mo	0.3298 (1)	0.7437 (1)	0.2690 (1)
S1	0.1996 (2)	0.7151 (3)	0.1853 (2)
S2	0.3726 (2)	0.9135 (4)	0.3670 (2)
N1	0.3299 (7)	0.6127 (13)	0.4394 (7)
N2	0.3177 (6)	0.9124 (12)	0.1043 (7)
C1	0.4011 (7)	0.5835 (16)	0.2874 (9)
C2	0.4026 (8)	0.6478 (16)	0.2244 (10)
C3	0.3253 (7)	0.6544 (15)	0.3775 (9)
C4	0.3234 (7)	0.8562 (13)	0.1655 (8)
C5	0.1363 (8)	0.6290 (16)	0.2311 (9)
C6	0.0561 (8)	0.6278 (19)	0.1591 (10)
C7	0.1287 (9)	0.7173 (17)	0.2976 (9)
C8	0.1645 (9)	0.4901 (15)	0.2599 (11)
C9	0.3885 (10)	1.0816 (15)	0.3347 (10)
C10	0.3145 (11)	1.1408 (17)	0.2735 (13)
C11	0.4507 (10)	1.0806 (18)	0.2966 (11)
C12	0.4162 (14)	1.1646 (23)	0.4150 (14)
C13	0.3418 (9)	0.5635 (16)	0.5208 (9)
C14	0.2706 (13)	0.5008 (34)	0.5169 (15)
C15	0.4063 (15)	0.4726 (30)	0.5477 (16)
C16	0.3629 (29)	0.6758 (31)	0.5789 (14)
C17	0.3082 (9)	0.9852 (14)	0.0283 (8)
C18	0.3393 (13)	0.8976 (22)	−0.0240 (12)
C19	0.2246 (11)	1.0202 (21)	−0.0151 (12)
C20	0.3560 (11)	1.1068 (18)	0.0526 (11)
C21	−0.0043 (23)	0.0210 (42)	0.0452 (20)
C22	0.0641 (25)	0.1018 (41)	0.1038 (26)
C23	0.0621 (21)	0.1398 (38)	0.1879 (22)
HC1	0.420 (9)	0.503 (16)	0.320 (9)
HC2	0.416 (10)	0.656 (19)	0.181 (10)
HC6A	0.049 (10)	0.721 (16)	0.146 (10)
HC6B	0.054 (9)	0.591 (15)	0.102 (10)
HC6C	0.031 (11)	0.597 (18)	0.185 (12)
HC7A	0.181 (7)	0.710 (13)	0.343 (8)
HC7B	0.106 (9)	0.815 (16)	0.278 (9)
HC7C	0.093 (6)	0.666 (12)	0.324 (7)
HC8A	0.178 (9)	0.440 (16)	0.210 (10)
HC8B	0.217 (9)	0.509 (15)	0.306 (9)
HC8C	0.126 (11)	0.471 (19)	0.276 (11)
HC10A	0.278 (8)	1.080 (14)	0.198 (9)
HC10B	0.274 (9)	1.160 (15)	0.304 (9)
HC10B	0.274 (9)	1.160 (15)	0.304 (9)
HC10C	0.327 (8)	1.236 (15)	0.260 (8)
HC11A	0.461 (9)	1.187 (16)	0.284 (9)
HC11B	0.496 (10)	1.062 (16)	0.347 (10)
HC11C	0.432 (9)	1.017 (16)	0.236 (10)
HC12A	0.439 (9)	1.259 (14)	0.413 (9)
HC12B	0.388 (9)	1.181 (15)	0.433 (9)
HC12C	0.461 (9)	1.130 (15)	0.459 (9)

[a] Standard deviations of the least significant figures are given in parentheses.

Table III. Fractional Coordinates for $Mo(t\text{-BuS})_2(t\text{-BuNC})_2(PhC{\equiv}CPh)$[a]

atom	x	y	z
Mo	0.2573 (1)	0.4762 (1)	0.3802 (1)
S1	0.3414 (2)	0.4683 (2)	0.2398 (3)
S2	0.2821 (2)	0.5612 (2)	0.5310 (3)
N1	0.1596 (6)	0.6295 (5)	0.2941 (8)
N2	0.3756 (5)	0.3364 (5)	0.4788 (7)
C1	0.1419 (6)	0.4390 (6)	0.3478 (9)
C2	0.1839 (7)	0.3840 (6)	0.3943 (9)
C3	0.1952 (6)	0.5752 (6)	0.3181 (9)
C4	0.3371 (6)	0.3876 (6)	0.4491 (9)
C5	0.3391 (7)	0.5451 (7)	0.1304 (9)
C6	0.4061 (9)	0.5206 (9)	0.0573 (11)
C7	0.3565 (9)	0.6238 (7)	0.1845 (11)
C8	0.2565 (8)	0.5470 (8)	0.0575 (11)
C9	0.3548 (8)	0.5349 (8)	0.6533 (10)
C10	0.4380 (7)	0.5221 (9)	0.6121 (11)
C11	0.3271 (9)	0.4628 (8)	0.7124 (11)
C12	0.3565 (10)	0.6063 (9)	0.7300 (11)
C13	0.1145 (9)	0.6999 (8)	0.2743 (11)
C14	0.0839 (11)	0.7069 (9)	0.1601 (13)
C15	0.0403 (10)	0.6919 (10)	0.3377 (15)
C16	0.1617 (11)	0.7595 (9)	0.3248 (15)
C17	0.4208 (7)	0.2699 (6)	0.5223 (10)
C18	0.4301 (12)	0.2151 (9)	0.4302 (12)
C19	0.4957 (9)	0.3013 (9)	0.5863 (15)
C20	0.3713 (10)	0.2336 (8)	0.6104 (12)
C21	0.0584 (6)	0.4542 (6)	0.3048 (10)
C22	0.0403 (7)	0.4744 (8)	0.1929 (10)
C23	−0.0408 (9)	0.4845 (9)	0.1526 (12)
C24	−0.0994 (8)	0.4768 (8)	0.2204 (12)
C25	−0.0828 (8)	0.4552 (8)	0.3335 (12)
C26	−0.0014 (7)	0.4438 (7)	0.3739 (10)
C27	0.1757 (7)	0.3031 (7)	0.4307 (11)
C28	0.1963 (10)	0.2436 (8)	0.3607 (13)
C29	0.1854 (10)	0.1669 (8)	0.3928 (14)
C30	0.1529 (10)	0.1537 (8)	0.4958 (15)
C31	0.1351 (11)	0.2085 (8)	0.5655 (15)
C32	0.1440 (9)	0.2886 (8)	0.5307 (12)

[a] Standard deviations of the least significant figures are given in parentheses.

to give a red oil, which was then chromatographed on a short alumina column with *n*-hexane as the eluent to yield a red solution. The volume was reduced to 3 mL and cooled at −30 °C overnight to give vermilion crystals of **2**: yield 0.30 mmol, 60%; mp 90 °C. Anal. ($C_{26}H_{42}N_2S_2Mo$) C, H, N.

Preparation of $Mo(t\text{-BuS})_2(t\text{-BuNC})_2(PhC{\equiv}CPh)$ (3). Solid $Mo(t\text{-BuS})_2(t\text{-BuNC})_4$ (0.5 mmol) and $PhC{\equiv}CPh$ (0.5 mmol) were placed in a flask under nitrogen. After toluene (20 mL) was added from a syringe, the deep yellow-green solution was stirred at 50 °C for 1 h, resulting in a deep red solution. Vacuum concentration to reduce volume to 3 mL was followed by addition of *n*-hexane (2 mL). Upon cooling at 30 °C overnight, deep rose red crystals of **3** (0.35 mmol, 70%) were obtained; mp 184 °C. Anal. ($C_{32}H_{64}N_2S_2Mo$) C, H, N.

X-ray Crystallographic Procedure. An orange-vermilion crystal of **1** grown from *n*-hexane and a deep rose red crystal of **3** grown from a toluene–*n*-hexane mixture (2:1) were carefully sealed in Lindemann capillaries under a nitrogen atmosphere and used to obtain X-ray data. The unit cell dimensions of **1** and **3** were obtained by least-squares refinement using the respective angular settings (35 reflections and 20 reflections) of each crystal. Intensity data were collected on automated diffractometers and were corrected for Lorentz and polarization factors, but no absorption correction was made. All measurements were made at ambient temperature. Table I summarizes the results of crystal data and data collection.

The structure of **1** was solved by the usual heavy-atom procedure: deconvolution of the Patterson function to reveal the Mo and the S positions and location of non-hydrogen atoms in subsequent electron density syntheses. The structure was refined by the block-diagonal least-squares technique, minimizing the function $\sum w(|F_o| - |F_c|)^2$; weights were assigned as $1.0/\sigma(F_o)^2$. R and R_w were 0.095 and 0.142 after five cycles of refinement with anisotropic temperature factors for Mo and S and isotropic factors for C and N atoms. At this stage, a hexane solvent molecule lying on a center of symmetry was found to be present in a successive difference map. Continued refinement of all non-hydrogen atoms resulted in $R = 0.075$ and $R_w = 0.083$. The hydrogen atoms associated with the acetylene and *t*-BuS groups were located on a difference map. Final full-matrix least-squares refinement of positional and anisotropic thermal parameters for non-hydrogen atoms and of positional parameters only for hydrogen atoms, to which isotropic temperature factors 1.0 Å^2 greater than those of the atoms bonded to them were assigned, led to convergence at $R = 0.059$ and $R_w = 0.066$.[24a] In the final least-squares cycle the shifts in all parameters were less than 0.3 esd.

(24) (a) Busing, W. R.; Martin, K. O.; Levy, H. A. "ORFLS, A Fortran Crystallographic Least Squares Program", U.S. Atomic Energy Commission Report ORNL-TM-305; Oak Ridge National Laboratory: Oak Ridge, TN, 1970. Johnson, C. A. "ORTEP-II, A Fortran Thermal Ellipsoid Plot Program for Crystal Structure Illustrations", U.S. Atomic Energy Commission Report ORNL-3794 (2nd revision with supplemental instructions); Oak Ridge National Laboratory: Oak Ridge, TN, 1971. Sakurai, T., Ed. "UNICS, The Universal Crystallographic Computation Program System"; The Crystallographic Society of Japan: Tokyo, Japan, 1967. (b) Germain, G.; Main, P.; Woolfson, M. M. *Acta Crystallogr., Sect. B* **1970**, *B26*, 274–285. Woolfson, M. M. *Acta Crystallogr., Sect. A* **1977**, *A33*, 219–225.

Table IV. Selected Electronic and IR Spectral Data of Mo(t-BuS)$_2$(t-BuNC)$_2$(RC≡CR′)

Electronic Spectra (in n-Hexane), λ_{max} (nm) (log ϵ)

1 (R = R′ = H)	2 (R = H, R′ = Ph)	3 (R = R′ = Ph)
265 (3.97)	271 (4.26)	280 sh (4.36)
300 sh (3.95)	314 (4.20)	287 sh (4.29)
324 (4.00)	345 sh (4.07)	297 sh (4.21)
346 sh (3.81)	457 (3.07)	315 (4.18)
452 (3.02)	552 (2.20)	350 sh (3.90)
546 (2.11)		461 (2.93)
		558 (2.15)

IR Spectra (cm^{-1})

	1		2		3	
	Nujol	hexane	Nujol	hexane	Nujol	hexane
ν(N≡C)	2105 vs	2095 vs	2140 m	2105 vs	2103 vs	2110 vs
	2065 sh	2060 sh	2105 vs	2070 sh	2060 sh	
			2050 m			
ν(MC$_2$)	1565 m		1672 m		1755 m	
$\Delta\nu$[a]	409		433		468	

[a] See text.

The structure of **3** was also solved by the heavy-atom method, combined with direct methods using the MULTAN program[24b] and refined for all non-hydrogen atoms by the block-diagonal least-squares technique as described in the preceding section. The final values were $R = 0.062$ and $R_w = 0.079$,[24a] respectively.

The neutral atomic scattering factors of Cromer and Waber[25] were used for non-hydrogen atoms, while those for H were from Stewart et al.[26] The real and imaginary corrections for anomalous dispersion were included for the Mo and S atoms.

Final atomic coordinates for **1** and **3** appear in Tables II and III, respectively. Temperature factors for **1** and **3** are available as supplementary material.

Results and Discussion

Formation. When acetylene gas was introduced into a deep yellowish green toluene solution Mo(t-BuS)$_2$(t-BuNC)$_4$ at 30 °C, the color soon turned to dark red. Two moles of t-BuNC was liberated in the reaction as detected by VPC:

$$\text{Mo}(t\text{-BuS})_2(t\text{-BuNC})_4 + \text{RC}{\equiv}\text{CR}' \xrightarrow[-2t\text{-BuNC}]{} \text{Mo}(t\text{-BuS})_2(t\text{-BuNC})_2(\text{RC}{\equiv}\text{CR}')$$

1, R = R′ = H
2, R = H, R′ = Ph
3, R = R′ = Ph

Similarly the reaction with PhC≡CH and PhC≡CPh occurs readily at 50 °C. **1** and **2** were purified by alumina chromatography with n-hexane as the eluent. **3** can be purified simply by recrystallization. The substitution reaction is selective; formation of lower valent Mo compounds was not detected in the reaction mixture even when more than 2 mol of alkynes was employed.

These alkyne complexes form crystals of varying red color which are moderately stable toward air and moisture. They show similar electronic spectra exhibiting several strong charge-transfer (CT) bands. The phenyl substituent on the alkyne ligand enhances the CT band intensity (Table IV).

IR Spectra. The alkyne and isocyanide ligands compete for electron transfer through their dπ–pπ* bondings. In late transition metal alkyne compounds containing alkyl isocyanides and an alkyne such as M(t-BuNC)$_2$(PhC≡CPh) (M = Ni, Pd), the alkyne ligand acts as a weak electron acceptor.[27,28]

Table V. ^{1}H and ^{13}C NMR Spectra of Mo(t-BuS)$_2$(t-BuNC)$_2$(RC≡CR′)

	1 (R = R′ = H)	2 (R = H, R′ = Ph)	3 (R = R′ = Ph)
	^{1}H NMR (δ, in C$_6$D$_6$)		
(CH$_3$)$_3$CNC	1.27 s	1.08 s, 1.28 s	1.10 s
(CH$_3$)$_3$CS	1.65 s	1.67 s	1.73 s
≡CH	10.43 s	10.40 s	
	^{13}C NMR (δ, in C$_6$D$_6$)		
(*C*H$_3$)$_3$CNC	30.3	29.7, 30.3	29.8
(CH$_3$)$_3$*C*NC	56.2	56.2	56.2
(CH$_3$)$_3$CN*C*	178.8		
(*C*H$_3$)$_3$CS	34.9	34.9	35.0
(CH$_3$)$_3$*C*S	44.5	45.0	45.4
≡*C*R	171.7	184.0,[b] 171.6[c]	183.4
$J_{\equiv CH}$, Hz	215	211	
$\Delta\delta$(≡C)[a]	95.7	100,[b] 93.9[c]	93.5

[a] $\Delta\delta$(≡C) = δ(free) − δ(coord). [b] Carbon adjacent to phenyl. [c] Terminal carbon.

Population analysis of the hypothetical compound Ni(NHC)$_2$(HC≡CH) shows electron drift from the isocyanide to the alkyne ligand,[29] reflecting an electron-widthdrawing property of acetylene somewhat stronger than that of alkyl isocyanide. In the case of early transition metal alkyne compounds, the situation is not obvious since an effective pπ–dπ donation would augment the pπ–dπ bonding.[11c,19] Let us examine the IR data. The IR N≡C stretching bands of **1**, **2**, and **3** appear in the region 2110–2060 cm^{-1}, which may be compared with those (2120 and 2010 cm^{-1}, in n-hexane) of the parent Mo(t-BuS)$_2$(t-BuNC)$_4$.[17] The frequencies increase in the order **1** < **2** < **3** (Table IV), manifesting an increase in electron transfer to the alkyne ligand and/or a decrease in pπ donation from the alkyne. Among the IR vibrational modes (2 a$_1$ + b$_1$) associated with metal–alkyne bonding (MC$_2$), only the highest frequency band, ν_1 (a$_1$), is generally observed,[19] because of extensive couplings of the lower frequency bands, ν_2 (a$_1$) and ν_3 (b$_1$):

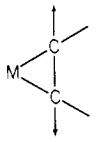

ν_1 (a$_1$)

The highest ν(MC$_2$) band appears in the region 1560–1760 cm^{-1}. Although this band is not a pure C≡C stretching vibration, the potential distribution function may be assumed to be heavily weighted on the C≡C stretching component. Thus it would be justifiable to use the difference ($\Delta\nu$) between ν(MC$_2$) and ν(C≡C) of the free alkyne as a rough measure of the perturbation the alkyne molecules receives upon coordination.

The $\Delta\nu$ value of Ni(t-BuNC)$_2$(PhC≡CPh) is 418 cm^{-1},[27] implying a greater reduction in C≡C bond order in Mo(II) (d^4) compounds than in Ni(0) (d^{10}) compounds, which involve essentially no pπ–dπ donation. These aspects might lead one to infer domination of pπ–dπ in the alkyne–Mo(II) bonding. Should this be true, from the trend of $\Delta\nu$ (**1** < **2** < **3**) one would expect a decrease in ν(NC) of isocyanide ligands in the order **1** > **2** > **3**. The observed trend is just the opposite (Table IV). Perhaps two t-BuS$^-$ ligands assist the dπ→pπ backbonding. In fact, the $\Delta\nu$ values, 409 and 468 cm^{-1}, found for

(25) Cromer, D. T.; Waber, J. T. "International Tables for X-ray Crystallography"; Ibers, J. A., Hamilton, W. C., Eds.; Kynoch Press: Birmingham, England, 1974; Vol. IV, Table 2.2A, p 72.
(26) Stewart, R. F.; Davidson, E. R.; Simpson, W. T. *J. Chem. Phys.* **1965**, *42*, 3175–3187.
(27) Otsuka, S.; Yoshida, T.; Tatsuno, Y. *J. Am. Chem. Soc.* **1971**, *93*, 6462–6469.
(28) Nakamura, A.; Yoshida, T.; Cowie, M.; Otsuka, S.; Ibers, J. A. *J. Am. Chem. Soc.* **1977**, *99*, 2108–2117.
(29) Tatsumi, K.; Fueno, T.; Nakamura, A.; Otsuka, S. *Bull. Chem. Soc. Jpn.* **1976**, *49*, 2170–2177.

1 and **3** respectively are greater than thsoe observed for a formally Mo(II) compound, $Mo(Cp)_2(RC{\equiv}CR)$,[9a] 361 and 449 cm^{-1} for R = H and R = Ph, respectively. The cis alignment of two *t*-BuS^- ligands in the equatorial plane possessing a perpendicular alkyne ligand, as revealed by the present X-ray analysis, is a geometry most favorable to support the $d\pi \rightarrow p\pi$ back-bonding. However, experimental assessment of the relative importance of the donative or retrodonative interactions appears to be difficult (see the MO analysis).

NMR Spectra. As shown in Table V, the methyl proton signal of the *t*-BuNC ligands of **1–3** appears in the region δ 1.27–1.10, which may be compared with the value δ 1.23 observed for the parent $Mo(t\text{-BuS})_2(t\text{-BuNC})_4$.[17] The methyl protons of the *t*-BuS ligands of **1–3** are somewhat more shielded than those (δ 1.98) of $Mo(t\text{-BuS})_2(t\text{-BuNC})_4$. Compound **2** shows two singlet signals corresponding to two

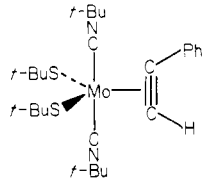

2

inequivalent *t*-BuNC ligands, which suggest a molecular structure similar to the structures of **1** and **3** established by the present X-ray analysis, namely, that the CC axis of PhC≡CH lies parallel to the molecular axis –NCMoCN–. Equilibration of the two isocyanide proton signals was not observed up to 100 °C. Because of considerable decomposition near 100 °C, the measurement at higher temperature was not attempted. Thus, **2** appears to be stereochemically rigid at least below 100 °C. The congeners **1** and **3** should behave similarly. The acetylenic proton signal of **1** and **2** appears at a very low field, around δ 10.4, yet the resonance is not as low as that (δ 13.05) of W(CO)(detc)(HC≡CH).[11b]

The ^{13}C NMR spectra are also shown in Table V. Consistent with ^1H NMR data, **2** shows two signals for the *t*-BuNC ligands, which do not equilibrate up to 100 °C. The chemical shift values of the *tert*-butyl carbons of both the *t*-BuNC and the *t*-BuS groups of **1–3** are comparable with those of the parent $Mo(t\text{-BuS})_2(t\text{-BuNC})_4$.[17] The signal of the isocyanide carbon bonded to the metal was not observed for **2** and **3** presumably due to the nuclear Overhauser effect. The chemical shift (δ 178.8) of the isocyanide carbons of **1** is similar to that (δ 174.8) of $Mo(t\text{-BuS})_2(t\text{-BuNC})_4$,[17] but the carbon atoms are more deshielded compared to those of some isocyanide Mo(II) compounds, for example, $[Mo(t\text{-BuNC})_6I]^+$ (δ 157.3 in $CDCl_3$, –35 °C[30]) and $[Mo(t\text{-BuNC})_4(t\text{-BuNHC}{\equiv}CNH(t\text{-Bu}))I]^+$ (δ 157.1 in $CDCl_3$[31]).

The ^{13}C signals of acetylenic carbons of **1–3** appear in the region δ 171–184 (Table V). According to the formalism proposed by King[15b] and Templeton,[11c] the alkyne ligands in **1–3** should be regarded as four-electron donors, which are expected to show the ^{13}C signal around δ 200. Note that, even with four electrons from the alkyne, **1–3** are 16-electron compounds. The correlation between δ and N (number of electrons donated by an alkyne ligand) would hold only for alkyne complexes involving auxiliary ligands capable of effective back-bonding such as CO, η-C_5H_5, etc. This is the same limitation the inert-gas rule also suffers.[21] It is not surprising that **1–3**, having the simple donor *t*-BuS^-, show considerable deviation from the tenet proposed by Templeton.

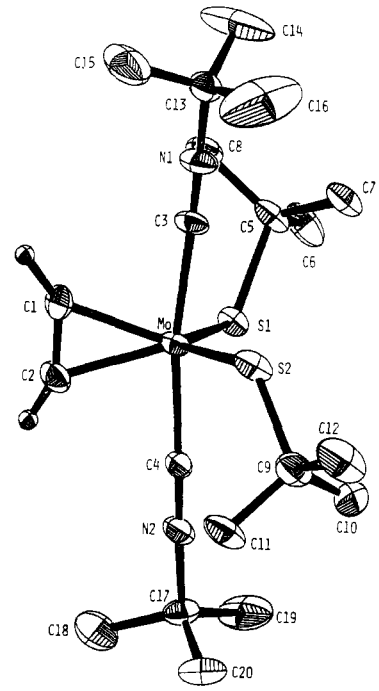

Figure 1. Perspective view of the molecule $Mo(t\text{-BuS})_2(t\text{-BuNC})_2(HC{\equiv}CH)\cdot{}^1/_2C_6H_{14}$ perpendicular to the plane Mo–C1–C2. The thermal ellipsoids are drawn at the 20% probability level, and hydrogen atoms are omitted for clarity except for the two atoms attached to the C1 and C2 atoms.

Table VI. Bond Distances (Å) of $Mo(t\text{-BuS})_2(t\text{-BuNC})_2(HC{\equiv}CH)\cdot{}^1/_2C_6H_{14}$ (**1**) and $Mo(t\text{-BuS})_2(t\text{-BuNC})_2(PhC{\equiv}CPh)$ (**3**)[a]

	1	3[b]		1	3[b]
Mo-S1	2.321 (3)	2.337 (3)	C5-C8	1.52 (2)	1.57 (2)
Mo-S2	2.329 (4)	2.338 (3)	C9-C10	1.51 (2)	1.57 (2)
Mo-C1	2.04 (2)	2.06 (1)	C9-C11	1.54 (3)	1.54 (2)
Mo-C2	2.05 (2)	2.05 (1)	C9-C12	1.53 (3)	1.55 (2)
Mo-C3	2.12 (2)	2.11 (1)	C13-C14	1.45 (3)	1.42 (2)
Mo-C4	2.09 (1)	2.15 (1)	C13-C15	1.44 (3)	1.55 (2)
S1-C5	1.87 (2)	1.87 (1)	C13-C16	1.47 (3)	1.40 (2)
S2-C9	1.85 (2)	1.86 (1)	C17-C18	1.53 (3)	1.48 (2)
N1-C3	1.12 (2)	1.14 (1)	C17-C19	1.49 (2)	1.51 (2)
N1-C13	1.43 (2)	1.45 (1)	C17-C20	1.48 (2)	1.56 (2)
N2-C4	1.17 (2)	1.14 (1)	C1-H1	0.9 (2)	
N2-C17	1.46 (2)	1.45 (2)	C2-H2	0.8 (2)	
C1-C2	1.28 (2)	1.28 (2)	C1-C21		1.48 (2)
C5-C6	1.54 (2)	1.57 (2)	C2-C27		1.48 (2)
C5-C7	1.51 (2)	1.53 (2)			

[a] The standard deviation of the least significant figure of each distance is given in parentheses. [b] The mean C–C distance of the phenyl groups is 1.40 (2) Å.

We will come back to this point later. It may be pertinent to point out here that the presence of the CO ligand(s), a powerful $d\pi$ acceptor, compensates well the effect of strong electron donation by *t*-BuS^-, as evidenced by the value δ 195.1 for a mercaptide-bridged Mo(I) dimer, $Mo_2(t\text{-BuS})_2(CO)_4(PhC{\equiv}CPh)_2$.[32]

Structure Description. The unit cell of **1** consists of individual monomeric units and *n*-hexane molecules with no unusual intermolecular contacts, while that of **3** consists of only the alkyne complex without solvent molecules. The phenyl substituents of adjacent molecules in **3** appear to align in close contact, but the shortest intermolecular phenyl atom nonbonded distance, between C26 and C26′, is 3.60 Å. The molecular axis of **1** is almost parallel to the (100) plane, while the axis of **3** is almost parallel to the (1$\bar{1}$0) or (110) plane.

(30) Lam, C. T.; Novotny, M.; Lewis, D. L.; Lippard, S. J. *Inorg. Chem.* **1978**, *17*, 2127–2133.
(31) Lam, C. T.; Corfield, P. W. R.; Lippard, S. J. *J. Am. Chem. soc.* **1977**, *99*, 617–618.
(32) Kamata, M.; Yoshida, T.; Otsuka, S.; Hirotsu, K.; Higuchi, T., to be submitted for publication.

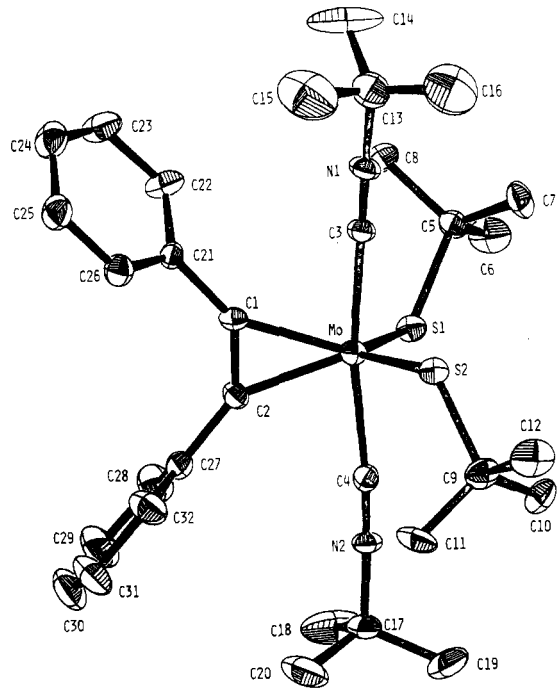

Figure 2. Perspective view of the molecule $Mo(t\text{-}BuS)_2(t\text{-}BuNC)_2(PhC{\equiv}CPh)$ perpendicular to the plane Mo–C1–C2. The thermal ellipsoids are drawn at the 20% probability level.

The molecular structures of the complexes **1** and **3** determined by the present X-ray diffraction studies are shown in Figures 1 and 2, respectively. The same numbering scheme was employed for both compounds except for the phenyl groups in **3**. The bond lengths and angles for **1** and **3** are listed in Tables VI and VII. The compounds **1** and **3** are almost isostructural, and each possesses approximately twofold symmetry. If the acetylene is regarded as an unidentate ligand, the environment of the Mo atom is best described as trigonal bipyramidal with two axial *t*-BuNC ligands, while the acetylene and two S atoms occupy the equatorial positions. The deviations of the Mo atoms from the equatorial plane are 0.019 (7) and −0.009 (4) Å in **1** and **3**, respectively. The most conspicuous feature is the parallel coordination of the acetylene triple bond with respect to the molecular axis C3–Mo–C4. Thus, the acetylene and isocyanide carbon atoms, C1, C2, C3, and C4, lie in the same plane within 0.02 (2) and 0.04 (1) Å for **1** and **3**, respectively. The molecular axis is slightly bent toward the two equatorial sulfur atoms, the C3–Mo–C4 angle being 170.7 (6)° for **1** and 170.6 (4)° for **3**. The (N≡)C–Mo–C(≡N) axis in the parent compound $Mo(t\text{-}BuS)_2(t\text{-}BuNC)_4$ also showed a similar bend (174.0 (3)°), but the direction is just reverse to that found in the present compounds.[17] The deviation of the C3–Mo–C4 angle from linearity in **1** and **3** may arise from repulsive interactions between acetylene and isocyanide carbon atoms. Thus, the nonbonded distances C1···C3 and C2···C4 are 2.58 (2) and 2.55 (2) Å for **1** and 2.58 (2) and 2.61 (2) Å for **3**, respectively; these values are far less than twice the van der Waals radius of a carbon atom (3.3 Å). The Mo–C3–N1 and Mo–C4–N2 axes in **1** and **3** are slightly bent (Table VII).

Another salient feature found in both **1** and **3** is the anti-upright alignment of the S–C bonds; this is in sharp contrast to the syn-upright alignment observed in the parent compound.[17] Probably due to a steric repulsion between the *t*-Bu groups of the isocyanide and thiolate ligands, the dihedral angles between the plane C3–Mo–C4 and the equatorial plane, 80.1 (3)° for **1** and 80.2 (8)° for **3**, deviate significantly from 90°. The long interatomic distances of S1···S2 (4.068 (5) Å for **1** and 4.083 (4) Å for **3**) compared to that (4.010 (3) Å) found in $Mo(t\text{-}BuS)_2(t\text{-}BuNC)_4$[17] are consistent with the wider S1–Mo–S2 angle (122.1 (2)° for **1** and 121.7 (1)° for **3**) compared to that (115.3 (1)°) in $Mo(t\text{-}BuS)_2(t\text{-}BuNC)_4$, although the mean Mo–S distance (2.325 (3)° for **1** and 2.338 (2) Å for **3**) is significantly shorter than that (2.373 (3) Å) of the latter.

The C≡C and the mean Mo–C(≡C) distances are 1.28 (2) and 2.054 (7) Å for **3** and 1.28 (2) and 2.05 (2) Å for **1**. These distances are intermediate between the corresponding values of $Mo(\eta\text{-}C_5H_5)_2(PhC{\equiv}CPh)$ (1.269 (7) and 2.143 (6) Å) and $Mo(EtDTC)_2(CO)(PhC{\equiv}CPh)$ (1.313 (4) and 2.039 (2) Å).[11]

Table VII. Bond Angles (deg) of $Mo(t\text{-}BuS)_2(t\text{-}BuNC)_2(HC{\equiv}CH)\cdot{}^1/_2C_6H_{14}$ (**1**) and $Mo(t\text{-}BuS)_2(t\text{-}BuNC)_2(PhC{\equiv}CPh)$ (**3**)[a,b]

	1	3
S1-Mo-S2	122.1 (2)	121.7 (1)
S1-Mo-C1	117.5 (4)	119.5 (3)
S1-Mo-C2	113.1 (4)	116.2 (3)
S1-Mo-C3	96.5 (3)	96.6 (3)
S1-Mo-C4	80.2 (3)	79.9 (3)
S2-Mo-C1	116.7 (4)	115.4 (3)
S2-Mo-C2	122.1 (4)	119.1 (3)
S2-Mo-C3	77.6 (4)	78.3 (3)
S2-Mo-C4	96.6 (4)	96.0 (3)
C1-Mo-C2	36.5 (7)	36.4 (4)
C1-Mo-C3	76.6 (6)	76.3 (4)
C1-Mo-C4	112.6 (6)	113.0 (4)
C2-Mo-C3	113.1 (6)	112.6 (4)
C2-Mo-C4	76.1 (6)	76.8 (4)
C3-Mo-C4	170.7 (6)	170.6 (4)
Mo-S1-C5	118.3 (4)	120.0 (4)
Mo-S2-C9	120.4 (6)	120.0 (4)
C3-N1-C13	175.5 (14)	174.8 (12)
C4-N2-C17	177.8 (15)	176.0 (11)
Mo-C1-C2	72.1 (10)	71.5 (7)
Mo-C2-C1	71.5 (11)	72.1 (7)
Mo-C3-N1	173.1 (11)	173.7 (10)
Mo-C4-N2	175.7 (11)	173.8 (9)
S1-C5-C6	103.7 (11)	104.0 (8)
S1-C5-C7	108.0 (11)	110.7 (8)
S1-C5-C8	112.0 (12)	110.7 (8)
S2-C9-C10	111.6 (12)	109.0 (8)
S2-C9-C11	111.0 (12)	110.7 (9)
S2-C9-C12	105.4 (14)	103.8 (9)
C6-C5-C7	106.0 (13)	111.2 (11)
C6-C5-C8	111.6 (13)	110.6 (10)
C7-C5-C8	114.8 (14)	109.6 (10)
C10-C9-C11	109.9 (16)	111.4 (11)
C10-C9-C12	108.6 (16)	110.4 (11)
C11-C9-C12	110.2 (16)	111.4 (11)
N1-C13-C14	108.2 (13)	111.1 (12)
N1-C13-C15	109.5 (18)	106.7 (11)
N1-C13-C16	107.9 (16)	106.7 (12)
N2-C17-C18	107.4 (13)	109.9 (10)
N2-C17-C19	108.4 (15)	106.0 (10)
N2-C17-C20	108.1 (11)	105.2 (10)
C14-C13-C15	111.9 (20)	104.8 (13)
C14-C13-C16	111.7 (27)	118.9 (14)
C15-C13-C16	107.5 (21)	108.1 (13)
C18-C17-C19	113.6 (13)	117.2 (13)
C18-C17-C20	108.9 (17)	111.0 (11)
C19-C17-C20	110.2 (14)	106.8 (11)
C1-C2-H2	148 (10)	
C2-C1-H1	152 (13)	
Mo-C1-C21		149.9 (8)
Mo-C2-C27		147.5 (8)
C1-C2-C27		140.3 (11)
C2-C1-C21		138.6 (11)
C1-C21-C22		118.7 (10)
C1-C21-C26		120.3 (10)
C2-C27-C28		119.0 (12)
C2-C27-C32		118.9 (11)

[a] The standard deviation of the least significant figure of each angle is given in parentheses. [b] The mean C–C–C angle of the phenyl groups is 120 (1)°.

The order of increasing acetylene–Mo(II) bond strength in these three Mo(II) complexes agrees well with a trend of increase in π-donation to the Mo atom as assessed by the MO calculations (vide infra). The mean bend-back angles of 30 (8) and 40.5 (8)° for **1** and **3** may be compared with those found in Mo(EtDTC)(CO)(PhC≡CPh) (39.7 (3)°)[11] and Mo(TPP)(PhC≡CPh) (39.3 (4)°),[9b] indicating that the angle is not sensitive to the alkyne–metal bond strength. The two aromatic rings in **3** are dissymmetrically disposed to the equatorial plane. The phenyl ring faces toward the *tert*-butyl group of each *t*-BuNC ligand.

Molecular Orbital Analyses on the Model $Mo(HS)_2(HNC)_2(HC{\equiv}CH)$. The aim of this section is a theoretical understanding of the electronic structure and the bonding of d^4 $Mo(t\text{-}BuS)_2(t\text{-}BuNC)_2(RC{\equiv}CR')$. For the trigonal-bipyramidal complexes, there are three geometrical features to be analyzed: (1) the orientation of acetylene, (2) the orientation of thiolates, and (3) the site preference of ligands, i.e. axial vs. equatorial (**4**). A simplified molecule, $Mo(HS)_2(HNC)_2(HC{\equiv}CH)$, was employed as the model for the extended Hückel calculations in this study.[33]

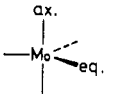

4

Given the stoichiometry, $Mo(A)(B)_2(C)_2$ (A = acetylene, B = thiolate, and C = isocyanide), with an ideal trigonal-bipyramidal arrangement, the five configurations **5–9** are

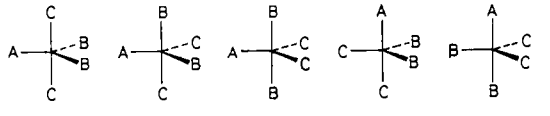

5 6 7 8 9

possible (without counting the enantiomer of **6**). Considering the conformational freedom of acetylene and thiolate ligands at an equatorial position, we examine the nine extreme structures. The **10a–10b**, **10′a–10′b**, and **12a–12b**, pairs are

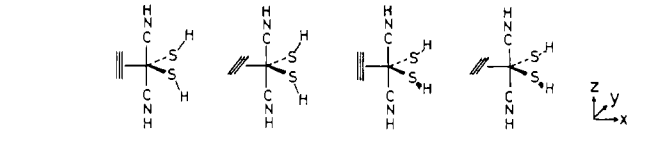

10a 10′a 10′b

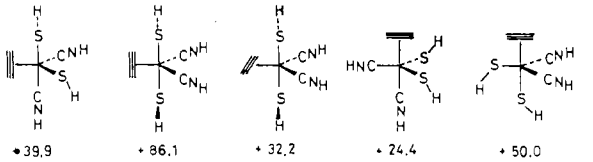

11 12a 12b 13 14

rotational isomers of an acetylene, while **10a**, **10b** and **10′a**, **10′b** represent the two typical orientations of thiolates. The total energies computed for the extreme geometries are compared in **10–14**, with a low-spin d^4 configuration assumed. The Mo–ligand distances and the S(eq)–Mo–S(eq) angles were taken from the observed structure of $Mo(t\text{-}BuS)_2(t\text{-}BuNC)_2(PhC{\equiv}CPh)$. The HNC(eq)–Mo–CNH(eq), HNC(eq)–Mo–SH(eq), and Mo–S–H angles were set at 120°.

(33) The extended Hückel parameters were taken from ref 17b.

The geometry **10a** was calculated to be most stable among the nine, which agrees with the observed structure of $Mo(t\text{-}BuS)_2(t\text{-}BuNC)_2$(alkyne). Two isocyanides tend to occupy the axial positions. Acetylene and two thiolates prefer the upright conformation at the equatorial coordination sites. The SH syn-upright conformer **15** was found to be as stable as **10a**. Steric and/or crystal-packing effects must be a reason that makes the molecule favor **10a** over **15**.

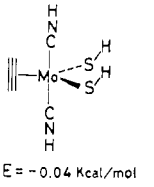

15

The site preference and stable conformations of ligands are explicable in terms of maximization of Mo–L π interactions.[34] The thiolate ligand is a π-donor through two nonequivalent lone pairs, in which the better donor is the pure 3p occupied orbital perpendicular to the M–S–R plane (**16**). The RNC

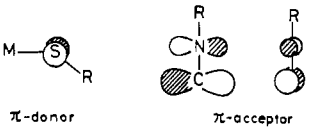

16 17

ligand can be regarded as a cylindrically symmetrical π-acceptor (**17**). Acetylene has two π and two π^* orbitals (**18**).

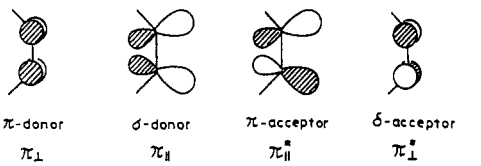

18

Of these, $\pi_\parallel^*$ acts as an acceptor in the M–L π interactions, while $\pi_\perp$ is able to donate electrons to the metal. We will discuss the M–π(acetylene) interactions in more detail later.

Let us suppose that the σ-donor strengths of thiolate, isocyanide, and acetylene are practically the same. Then the expected d-level splitting scheme for the trigonal-bipyramidal molecule is a "one-above-two-above-two" as shown in **19**, in

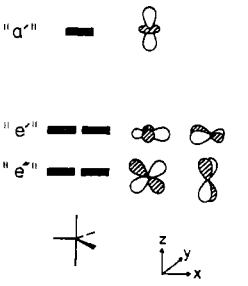

19

which π bonding from the ligands is assumed absent. Electrons in a d^4 system occupy the lowest "e" orbitals leaving the "e′" and "a_1′" vacant. The high-lying "a_1′" has nothing to do with the π interactions. Thus π donor ligands choose coordination sites and tend to orient themselves so as to achieve the maximal interaction with the vacant "e′" orbitals. On the other hand, π acceptors tend to find overlaps with the occupied "e″" or-

(34) Detailed theoretical analyses on pentacoordinated transition-metal complexes are given in: Rossi, A. R.; Hoffmann, R *Inorg. Chem.* **1975**, *14*, 365–374.

Table VIII. Relative Energies of the Extreme Conformations Calculated for Various d-Electron Counts

conformation	rel energy, ΔE, kcal/mol[a]			
	d^2	d^4	d^6	d^8
10a	*0.0*	*0.0*	47.9	63.4
10b	9.73	9.94	*0.0*	4.47
10'a	6.68	24.9	54.4	59.6
10'b	4.02	22.6	17.6	3.09
11	36.5	39.9	49.9	18.4
12a	70.6	86.1	81.9	75.6
12b	21.9	32.2	15.6	*0.0*
13	6.50	24.4	40.7	41.1
14	32.3	50.0	59.7	48.3

[a] Energies relative to the most stable conformation of a given d-electron count. Ground singlet configurations are assumed.

bitals. With these basic rules we can easily rationalize the structure of d^4 $Mo(RS)_2(RNC)_2$(alkyne). The axial positions are ideal for the cylindrically symmetrical acceptor, RNC, because two orthogonal π-acceptor orbitals interact with two d orbitals of e'' symmetry. The π donor, RS, is happy at the equatorial position with an upright conformation. For acetylene, the in-plane conformation at an equatorial site such as **10b** is obviously not a good geometrical choice. If we take only the $\pi_{\parallel}^*$-acceptor character of acetylene into account, there is no effective discrimination between axial and equatorial-upright coordination modes. However the $\pi_{\perp}$–d interaction makes a distinction between the two modes. The occupied $\pi_{\perp}$ orbital finds one of the vacant "e'" d orbitals to interact with, only in an equatorial-upright geometry.

We have shown that the observed geometry **10a**, which is also calculated to be most stable, is optimum in terms of Mo–L π interactions. The π interactions stabilize "e''" and destablize "e'" by different amounts, giving the HOMO–LUMO energy gap of 1.75 eV. The frontier molecular orbitals of **10a** are shown at the left side of Figure 3. The relatively large energy gap is consistent with the observed diamagnetism of $Mo(RS)_2(RNC)_2$(alkyne).

As one might expect, the orientations and the site preferences are sensitive to the number of d electrons. Table VIII shows relative total energies of the nine extreme geometries for various d-electron counts.[35] Ground singlet configurations are again assumed for the calculations. For d^2, as for the d^4 system, **10a** is most stable. Geometries **10'b** and **13** are less stable but not by much. In the d^8 case, the most stable geometry becomes **12b**, while **10b** and **10'b** are stable as well. At the center and the right side of Figure 3 we show the frontier molecular orbitals of the two conformations **10b** and **12b**, respectively. These two structures can be interconverted by a Berry pseudorotation plus a simultaneous acetylene rotation (**20**). The pseudorotation is an allowed process for

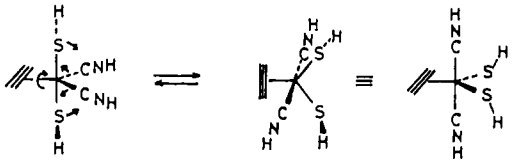

20

low-spin d^8 species in terms of the orbital symmetry rule.[34,36] In either of the structures, a coordinated alkyne will prefer an in-plane orientation to an upright one. This is indeed the conformation found in related d^8 trigonal-bipyramidal com-

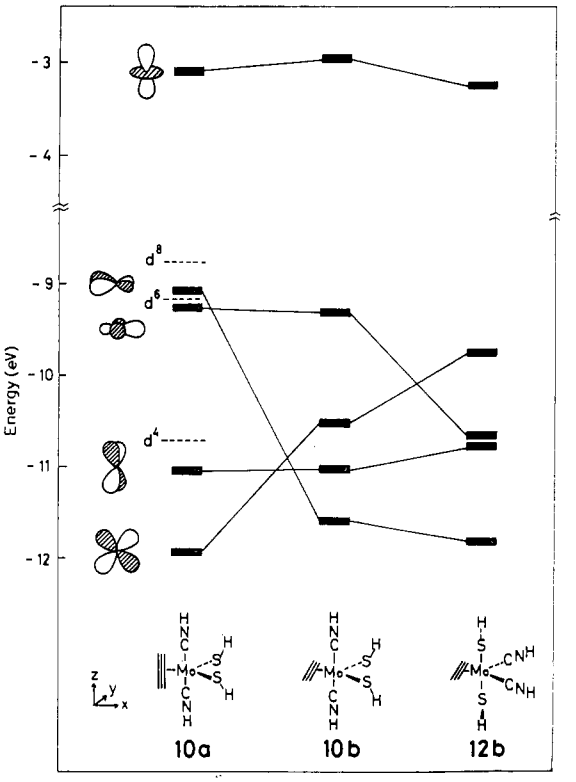

Figure 3. d-Orbital energy levels of three typical geometries of $Mo(SH)_2(CNH)_2(HC{\equiv}CH)$.

plexes,[37] e.g. **21**[37a] and **22**.[37b] Examples of the olefin analogue are many.[38]

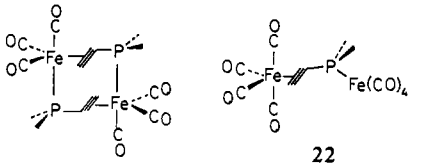

21 **22**

The most interesting aspect of Table VIII is that an addition of two electrons to d^4 $Mo(RS)_2(RNC)_2$(alkyne) rotates an alkyne from the upright conformation **10a** to the in-plane conformation **10b** with the geometry of other ligands fixed. Such a situation of six d electrons can be achieved in two distinct ways. One can doubly reduce $Mo(RS)_2(RNC)_2$(alkyne) (**23**). Or one can move to another

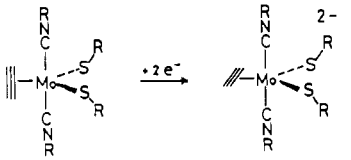

23

metal such as Fe, Ru, or Os. The reader might suspect that the d^6 $M(RS)_2(RNC)_2$(alkyne) molecules could have triplet

(35) Square pyramids, in which acetylene sits at the axial position, were calculated to be less stable than the most stable conformation of trigonal-bipyramidal structure for any of the d-electron counts.

(36) Eaton, D. R. *J. Am. Chem. Soc.* **1968**, *90*, 4272–4275.

(37) (a) Carty, A. J.; Paik, H. N.; Palenik, G. J. *Inorg. Chem.* **1977**, *16*, 300–305. (b) Carty, A. J.; Smith, W. F.; Taylor, N. J. *J. Organomet. Chem.* **1978**, *146*, C1–4. (c) Davies, B. W.; Puddephatt, R. J.; Payne, N. C. *Can. J. Chem.* **1972**, *50*, 2276–2284. (d) Davies, B. W. Payne, N. C. *Inorg. Chem.* **1974**, *13*, 1843–1848. (e) Kirchner, R. M.; Ibers, J. A. *J. Am. Chem. Soc.* **1973**, *95*, 1095–1101.

(38) See, for example: (a) Barborak, J. C.; Dasher, L. W.; McPhail, A. T.; Nichols, J. B.; Onan, K. D. *Inorg. Chem.* **1978**, *17*, 2936–2943. (b) Pinkerton, A. A.; Carrupt, P. A.; Vogel, P.; Boschi, T.; Thuy, N. H.; Roulet, R. *Inorg. Chim. Acta* **1978**, *28*, 123–132. Also see references in ref 37a and in: (c) Albright, T. A.; Hoffmann, R.; Thibeault, J. C.; Thorn, D. L. *J. Am. Chem. Soc.* **1979**, *101*, 3801–3812.

ground states, judging from the basic d-orbital splitting pattern of a trigonal-bypyramidal structure (**20**).[39] However, M–L π interactions rearrange the orbital energy levels, providing a relatively large HOMO(xz)–LUMO(x^2-y^2) energy gap for the geometry **10b**. In our calculations the energy gap amounts to 1.21 eV. Although π-donor substituents of the alkyne may push the HOMO up through a π–xz interaction, we think that d^6 $Mo(RS)_2(RNC)_2(alkyne)^{2-}$ has a good chance of having a singlet ground state.

Returning to d^4 $Mo(RS)_2(RNC)_2(alkyne)$, we examine the alkyne rotational barrier for **10a** → **10b** → **10a**. The ^1H and ^{13}C NMR spectra of $Mo(t\text{-}BuS)_2(t\text{-}BuNC)_2(PhC{\equiv}CH)$ show that the upright geometry of the alkyne is rigid up to 100 °C. In a model calculation on $Mo(HS)_2(HNC)_2(HC{\equiv}CH)$, varying the angle α of **24** from 0° (**10a**) to 90° (**10b**), we

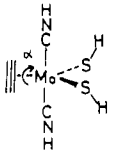

24

calculate a barrier of 10.4 kcal/mol. An energy maximum comes at α = 85°, and not at α = 90°, for the rigid rotation. The calculated barrier is somewhat smaller than what we would expect from the experimental result. Our simplified model, of course, lacks the steric bulk of *tert*-butyl and phenyl groups, which may be one factor in the geometrical rigidity of $Mo(t\text{-}BuS)_2(t\text{-}BuNC)_2(PhC{\equiv}CH)$.

Although the calculated barrier is rather small, we should point out that one of the two occupied levels changes its nature in going from **10a** to **10b**. As can be seen in Figure 5, the two highest occupied orbitals of **10a** are comprised mainly of xz and yz, while "xy" and "yz" are occupied in **10b**. The molecule maintains only the C_2 symmetry so that the "xz" and "xy" orbitals do actually avoid a crossing during the acetylene rotation. However, a certain amount of an "orbital-symmetry-forbidden" character must be retained. This is, we think, a reason for the presence of the energy maximum at α = 85° and for the rigidity of the acetylene upright orientation.

Now we bring Mo–alkyne interactions into focus. The filled alkyne $\pi_\perp$ orbital may play an important role in the metal–alkyne linkage of some mononuclear transition-metal complexes.[4b,9b,11c,15b,40] The observed ^{13}C chemical shift of δ 171–184 contrasts well with the shift of δ 115–118 for $(Cp)_2Mo(alkyne)$, in which the alkyne behaves as a two-electron donor, but is certainly smaller than what one would expect for a four-electron-donor alkyne. In order to explain the observed chemical shifts, we performed population analyses on $Mo(HS)_2(HNC)_2(HC{\equiv}CH)$ (**10a**). The amount of electron transfer from $\pi_\perp$ to the Mo site is calculated to be 0.223e, while the σ donation from $\pi_\parallel$ and the π back-donation to $\pi_\parallel$* are 0.296e and 0.584e, respectively. Obviously the $\pi_\perp$–Mo interaction is significant, and its magnitude is comparable to that of the $\pi_\parallel$–Mo interaction. Calculations were next carried out on $Mo(CO)(S_2CNH_2)_2(HC{\equiv}CH)$ and $(Cp)_2Mo(HC{\equiv}CH)$ with geometrical parameters of the Mo–HC≡CH portion fixed. The former molecule is the model for $Mo(CO)(dmtc)_2(PhC{\equiv}CPh)$, a typical example where the alkyne acts as a four-electron donor. We calculate the $\pi_\perp$ → Mo donation to be 0.260e for $Mo(CO)(S_2CNH_2)_2(HC{\equiv}CH)$ and 0.146e for $(Cp)_2Mo(HC{\equiv}CH)$. The ordering of $\pi_\perp$ donations is $Mo(S_2CNH_2)_2(CO)(HC{\equiv}CH)$ > $Mo(HS)_2(HNC)_2(HC{\equiv}CH)$ > $Mo(Cp)_2(HC{\equiv}CH)$, agreeing well with the ^{13}C chemical shifts observed for the corresponding alkyne complexes. Our analysis traces the trend to the energy of the xy orbital in each Mo moiety, which is responsible for accepting electrons from the acetylene $\pi_\perp$ orbital.[41] This is shown in **25**. As the $\pi_\perp$ energy level (−13.36

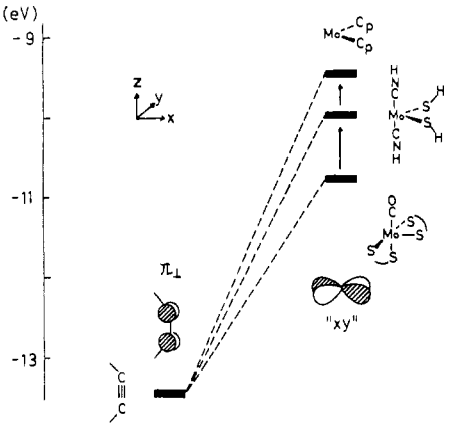

25

eV) is always lower than the xy level, the raising of xy weakens the π–"xy" interaction. The xy orbital of the $Mo(HS)_2(HNC)_2$ fragment is indeed lower than that of $(Cp)_2Mo$ but is destabilized in comparison with $Mo(CO)(S_2CNH_2)_2$ "xy". The destabilization is a consequence of a strong σ donation by thiolates at an equatorial plane.

Acknowledgment. The authors are grateful to Prof. R. Hoffmann for stimulating discussions. K.T. was generously supported by the National Science Foundation through Research Grant CHE 7828048 at Cornell University. We thank the Crystallographic Research Center, Institute for Protein Research, of Osaka University and the Computer Center of Osaka City University for computer calculations.

Registry No. **1**, 79803-04-6; **2**, 79803-05-7; **3**, 79681-75-7; $Mo(t\text{-}BuS)_2(t\text{-}BuNC)_4$, 77593-55-6.

Supplementary Material Available: Tables of temperature and structure factors for **1** and **3** and figures of their crystal structures (19 pages). Ordering information is given on any current masthead page.

(39) A d^6 trigonal-bipyramidal complex, $Co(P(C_2H_5)_3)_2Cl_3$, exhibits a triplet spin state: Jensen, K. A.; Nygaard, B.; Pedersen, C. T. *Acta Chem. Scand.* **1963**, *178* 1126–1132. van Enckevort, W. J. P.; Hendriks, H. M.; Beurskens, P. T. *Cryst. Struct. Commun.* **1977**, *6*, 531–536.

(40) Cotton, F. A.; Hall, W. T. *J. Am. Chem. Soc.* **1979**, *101*, 5094–5095.

(41) Of course a spatial extention of "xy" toward acetylene, i.e. pd hybridization, is another factor that affects the magnitude of π–"xy" interaction. For simplicity, however, we do not discuss the pd hybridization in this paper. The importance of the "xy" energy level was demonstrated in: Tatsumi, K.; Hoffmann, R.; Templeton, J. L. *Inorg. Chem.* **1982**, *21*, 466–468.